

# Body shape transformation along a shared axis of anatomical evolution in labyrinth fishes (Anabantoidei)

David C. Collar,<sup>1,2</sup> Michelle Quintero,<sup>3</sup> Bernardo Buttler,<sup>3</sup> Andrea B. Ward,<sup>4</sup> and Rita S. Mehta<sup>3</sup>

<sup>1</sup>Department of Organismal and Environmental Biology, Christopher Newport University, Newport News, Virginia 23606

<sup>2</sup>E-mail: david.collar@cnu.edu

<sup>3</sup>Department of Ecology and Evolutionary Biology, University of California, Santa Cruz, California 95060

<sup>4</sup>Department of Biology, Adelphi University, Garden City, New York, 11530

Received June 26, 2015

Accepted February 1, 2016

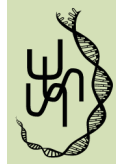
Major morphological transformations, such as the evolution of elongate body shape in vertebrates, punctuate evolutionary history. A fundamental step in understanding the processes that give rise to such transformations is identification of the underlying anatomical changes. But as we demonstrate in this study, important insights can also be gained by comparing these changes to those that occur in ancestral and closely related lineages. In labyrinth fishes (Anabantoidei), rapid evolution of a highly derived torpedo-shaped body in the common ancestor of the pikehead (*Luciocephalus aura* and *L. pulcher*) occurred primarily through exceptional elongation of the head, with secondary contributions involving reduction in body depth and lengthening of the precaudal vertebral region. This combination of changes aligns closely with the primary axis of anatomical diversification in other anabantoids, revealing that pikehead evolution involved extraordinarily rapid change in structures that were ancestrally labile. Finer-scale examination of the anatomical components that determine head elongation also shows alignment between the pikehead evolutionary trajectory and the primary axis of cranial diversification in anabantoids, with much higher evolutionary rates leading to the pikehead. Altogether, our results show major morphological transformation stemming from extreme change along a shared morphological axis in labyrinth fishes.

**KEY WORDS:** Axial skeleton, elongation, gourami, *Luciocephalus*, pikehead, rate of evolution.

Evolution proceeds at an uneven pace across the tree of life. Changes in form can be persistently rapid in some clades, perhaps following functional innovation (Price et al. 2010), ecological opportunity (Seehausen 2006; Losos 2009; Mahler et al. 2010), or both (Wagner et al. 2012); it can remain slow in others, such as in so-called nonadaptive radiations (Wake et al. 1983; Kozak et al. 2006); or it can vary within clades depending on aspects of species' ecology (Collar et al. 2009, 2010; Martin and Wainwright 2011; Price et al. 2011). However, occasionally during the course of evolution, a major burst of change occurs in a single lineage and leads to descendants that differ markedly from their close relatives. A classic example of this phenomenon is the evolution of elongate body form, which punctuates diversification in several vertebrate radiations including ray-finned

fishes (Jansen et al. 2006; Ward and Brainerd 2007; Claverie and Wainwright 2014), lissamphibians (Wake 1966; Wake 1980; Parra-Olea and Wake 2001), and squamates (Gans 1975; Wiens and Singluff 2001; Wiens et al. 2006; Brandley et al. 2008). Major transformations such as these have long fascinated evolutionary biologists because they contribute disproportionately to morphological diversity and stand in stark contrast with patterns of finer-scale change in closely related species (McPeck 1995; Ricklefs 2005; Wiens et al. 2006; Bergmann and Irschick 2012).

How do these bursts of evolution occur from within what appear to be more constrained clades? A satisfying answer to this question ultimately requires an integrated understanding of genetics, development, and historical selection. However, before



such a synthetic perspective is possible, it is first necessary to identify the specific anatomical changes underlying the transformation, which is typically accomplished by comparing ancestral to derived character states. Documenting the anatomical basis of transformation can help identify potential intrinsic (i.e., genetic, developmental, or functional) constraints on evolution or extrinsic selective factors and can even point to shared aspects of anatomical evolution when a transformation is replicated across lineages (Wiens et al. 2006; Ward and Brainerd 2007; Bergmann et al. 2009; Maxwell and Wilson 2013). Nevertheless, a key question that has received relatively little attention is how the structural changes underlying major transformations compare to ancestral patterns of evolution. In other words, are transformations the product of exaggerated changes in structures that are ancestrally labile or do they involve wholly novel combinations of structural change?

Bursts of evolution in form might be most likely to occur when the underlying structures are ancestrally evolutionarily changeable. This hypothesis is inspired by several influential studies demonstrating that between-species divergence is shaped by within-species (or within-population) variation, or in other words, that species diversify along genetic or developmental “lines of least resistance” (e.g., Schluter 1996; Hansen and Houle 2008; Hohenlohe and Arnold 2008). Our hypothesis is the macroevolutionary analog; major morphological transformations may occur along “anatomical lines of least resistance,” or the main axes of anatomical change in ancestral lineages. There are two nonexclusive reasons to expect this alignment. First, the readiness of structures to diverge is known to reflect genetic, developmental, or functional constraints that determine available phenotypic variation on which natural selection acts (Olson and Miller 1965; Schluter 1996; Stepan et al. 2002; Klingenberg 2008), and these constraints are likely to be passed from ancestral to descendent lineages. Rapidly evolving species may therefore experience the same biases in structural evolution as closely related, routinely evolving species. Second, if environmental conditions are shared broadly among members of a clade, species may share features of the adaptive landscape, and morphological transformation may represent adaptation toward one extreme of a selective axis along which ancestral species have already been diverging.

Alternatively, major transformations may result from evolutionary processes that deviate from those that lead to routine between-species divergence. Events such as population bottlenecks, mutations in regulatory or pattern-forming genes with large phenotypic effect, or some combination of these can cause major structural changes that differ from the pattern of evolution exhibited within the clade from which it is derived (Simpson 1953; Mayr 1963; Futuyma 1987; Davidson and Erwin 2006).

Our study examines the evolution of body shape, which is a fundamental aspect of ray-finned fish diversification. Specifically, we describe transformations along a continuum of body elongation from disc-shaped to torpedo-shaped forms. This elongation continuum describes one of the most conspicuous axes of morphological diversity in fishes, both among and within disparate teleost clades (Ward and Brainerd 2007; Maxwell and Wilson 2013; Claverie and Wainwright 2014). Body shape also has profound consequences for many aspects of fish biology, as it influences swimming kinematics and performance (Webb 1982, 1984), habitat use (Nelson 2006; Yamada et al. 2009), as well as feeding physiology (Mehta and Wainwright 2007; Ward and Kley 2012) and behavior (Mehta et al. 2010). A variety of anatomical changes have been shown to drive transformation of body shape; overall body elongation can occur through any combination of reduction in length of the secondary body axis, elongation of the head, or lengthening of the precaudal and/or caudal regions of the axial skeleton (Ward and Brainerd 2007; Collar et al. 2013). Moreover, change in a particular body region can result from modifications to any of several component structures. For example, elongation of axial skeleton regions can occur through increases in the number of vertebrae or their length (Parra-Olea and Wake 2001; Ward and Brainerd 2007; Ward and Mehta 2010).

We describe body shape variation in the Anabantoidei, or labyrinth fishes, which is a prominent perciform radiation of about 140 species found in the freshwaters of Asia and Africa. All species in this group possess a labyrinth organ, a modified and highly vascularized epibranchial bone that allows these fish to breathe air (Peters 1978; Liem 1980). Partly because of this capacity, species of this clade occupy a variety of habitat types and exhibit varied body shapes, including deep-bodied forms (e.g., the kissing gouramis, *Helostoma temminckii*) and more fusiform shapes (e.g., some climbing gouramis, like *Anabas*). However, this clade also includes two species, *Luciocephalus aura* and *L. pulcher* (pikehead), whose torpedo-shaped body resembles that of the distantly related pike (*Esox*) or pike characin (*Boulengerella*). In fact, *Luciocephalus* deviates so drastically from other labyrinth fishes that early systematists excluded it from Anabantoidei (Gray 1831) or classified it as the sister group to all other anabantoids (Lauder and Liem 1983), though it has since been definitively shown to be nested well within Anabantoidei (Britz 1994; Rüber et al. 2006). In this study, we apply a robust phylogeny for labyrinth fishes (Rüber et al. 2006) and use phylogenetic comparative methods to address three primary questions about body shape evolution within this clade: (1) Does evolution of the *Luciocephalus* morphology represent a major morphological transformation? (2) If so, what anatomical changes are responsible for the extreme shift in body form? (3) Do these changes align with the primary axis of diversification exhibited in other labyrinth fishes?

## Methods

### QUANTIFYING BODY SHAPE AND ITS ANATOMICAL BASIS

To quantitatively describe body shape and the anatomical components that contribute to it, we applied an index of shape variation—the vertebrate shape index (*VSI*)—that we developed in a prior study (Collar et al. 2013). *VSI* describes a continuum of body shape from disc- or football-shaped bodies to elongate forms and is the sum of shape in four distinct anatomical regions:

$$VSI = A_2 + H + PC + C, \quad (1)$$

where  $A_2$  describes the length of the secondary axis of the body (depth or width, whichever is longer),  $H$  is head shape, and  $PC$  and  $C$  describe the length of the precaudal and caudal regions of the vertebral column, respectively (note that these regions can be distinguished by the presence or absence, respectively, of a fused haemal arch; Grande and Bemis 1998; Ward and Brainerd 2007). All body region variables are proportional to their degree of elongation—their length in the primary (anteroposterior) body axis relative to the secondary (dorsoventral or lateral) axis. *VSI* therefore allowed us to quantify overall body elongation in species and to examine the contribution of separate anatomical components to variation in shape.

We quantified *VSI* for 24 labyrinth species representing some of the most morphologically divergent species from each of the major phylogenetic lineages of Anabantoidei identified in a recent phylogenetic analysis (Rüber et al. 2006). For each species, we sampled between one and eight individuals (median = 4 individuals;  $N \geq 3$  for 18 species). Body region morphology was determined by measurements of several structures:  $A_2$  is the ratio of the lengths of the primary (anteroposterior;  $L_1$ ) and secondary ( $L_2$ ) body axes (in this case,  $L_2$  is body depth, and its measurement excludes the dorsal, anal, and pelvic fins);  $H$  is the product of the length of the head ( $L_H$  = the number of vertebrae equal to the length of the skull) and its aspect ratio ( $AR_H$  = ratio of skull length in the primary and secondary body dimensions); vertebral ( $PC$  or  $C$ ) elongation is the product of the number of vertebrae ( $N_{PC}$  or  $N_C$ ) and mean aspect ratio (i.e., the ratio of centrum length along the primary and secondary body axes;  $AR_{PC}$ ,  $AR_C$ ) of individual vertebrae. For 21 of the 24 species, specimens were cleared and double stained for bone and cartilage (Song and Parenti 1995) and measurements were made using digital calipers or, for smaller specimens, an ocular micrometer fitted to a Nikon dissecting microscope. For the remaining three species, we measured bone dimensions on digital radiographs from the Museum of Comparative Zoology at Harvard University. Specimen information and species values for *VSI* and its body region components are in Table S1, and morphological measurements per specimen are available in the Dryad Digital Repository (Collar et al. 2016).

Further details regarding measurement methods, including landmarks for linear measurements and protocols for counting vertebrae, can be found in Collar et al. (2013). Species values were log-transformed to homogenize variance across values of all variables.

### TESTING FOR EXTREME MORPHOLOGICAL EVOLUTION IN *LUCIOCEPHALUS*

We used a phylogenetic comparative approach to assess whether body shape evolution leading to *Luciocephalus* was exceptionally fast compared to other anabantoids. We fit evolutionary models to *VSI* data for species given a phylogenetic tree. We recreated the phylogenetic reconstruction of Rüber et al. (2006) using their aligned DNA sequence matrix, which we downloaded from TreeBase (treebase.org, matrix accession no. M2523, study accession no. 1464). This dataset includes 58 anabantoid species plus two *Channa* species as the outgroup. We reanalyzed the Rüber et al. (2006) sequence data instead of using their summary tree to generate a sample of trees that would allow us to account for phylogenetic uncertainty in our analyses (Huelsenbeck and Rannala 2003; see below). Details of our phylogenetic methods are described in Supporting Information Methods, but we note that we used Bayesian phylogenetic analysis implemented in *BEAST* (Drummond and Rambaut 2007) to simultaneously reconstruct phylogenetic relationships and estimate branch lengths in relative time (Drummond et al. 2006). The resulting trees were in close agreement with phylogeny estimation of Rüber et al. (2006). We pruned trees to include only the 24 anabantoid species in our morphological dataset, which represents relatively even sampling of anabantoid subclades. All phylogenetic comparative analyses were performed on the maximum clade credibility (MCC) tree and repeated on a sample of 100 trees from the posterior probability distribution.

To test whether the ancestral *Luciocephalus* lineage experienced exceptionally rapid body shape evolution, we used maximum likelihood to fit a Brownian motion model of evolution that allows the rate of *VSI* evolution on the phylogenetic branch leading to the two *Luciocephalus* species to differ from the rate in other anabantoids (see Fig. 1). We then compared this model to a single-rate Brownian model that constrained all anabantoid lineages to the same rate. This procedure follows the methods of Revell (2008) and O'Meara et al. (2006), which are implemented in the function *brownie.lite* in the *phytools* package (Revell 2012) for the R statistical computing environment (R Core Development Team 2015). To assess support for the two-rate model we compared small sample size corrected Akaike Information Criteria (AICc) for the full (two-rate) and constrained (one-rate) models (Burnham and Anderson 2002). We then compared evolutionary rates in the *Luciocephalus* ancestor and other anabantoids using model averaged estimates (i.e., mean rate across models weighted

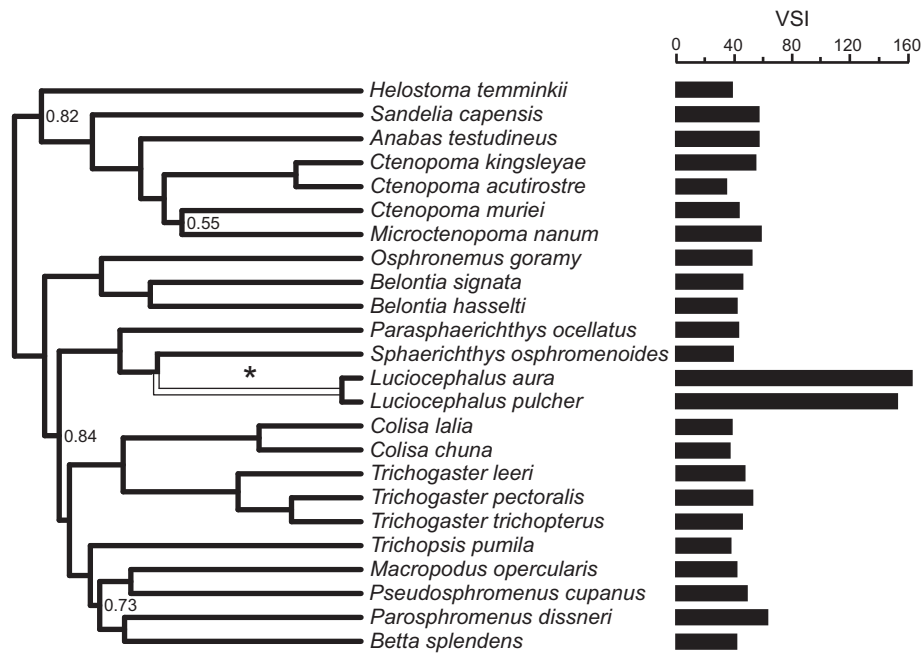


**Figure 1.** Phylogeny for 24 anabantoid species and their VSI values. Phylogeny is the maximum clade credibility tree from a Bayesian phylogenetic analysis modeled after Rüber et al. (2006). Branch lengths are proportional to time (i.e., total tree depth = 1.0), and nodes are supported by greater than 0.90 Bayesian posterior probabilities unless otherwise indicated. The phylogenetic branch representing the common ancestor of the two *Luciocephalus* species (*L. aura* and *L. pulcher*) is highlighted in white and marked with an asterisk. We tested for exceptional evolution in the ancestral *Luciocephalus* lineage by allowing the evolutionary rate along this branch to differ from the evolutionary rate along the remaining anabantoid branches. Black bars next to species names are proportional to the mean VSI measured for that species with scale bar shown at the top.

by the AIC weight [AICw] of each model; Burnham and Anderson 2002).

To determine which body regions are responsible for the shift in VSI in *Luciocephalus*, we repeated the above model-fitting and model-averaging analyses separately for secondary axis reduction ( $A_2$ ), head elongation ( $H$ ), and precaudal ( $PC$ ) and caudal ( $C$ ) elongation. Body regions that showed substantially elevated rates in the *Luciocephalus* ancestor were interpreted as important in driving the body shape transformation.

### COMPARING ANATOMICAL CHANGE IN *LUCIOCEPHALUS* TO OTHER ANABANTOIDS

We tested whether the suite of anatomical changes leading to *Luciocephalus* aligned with the primary axis of diversification in other anabantoids. Our method involved reconstructing the evolutionary trajectory leading to the most recent common ancestor (MRCA) of *Luciocephalus*, estimating the primary axis of diversification in other anabantoids, and comparing the alignment of these axes to the alignment expected when evolutionary rates and covariances are constant among all anabantoid lineages.

To reconstruct evolutionary change in body regions ( $A_2$ ,  $H$ ,  $PC$ , and  $C$ ) along the phylogenetic branch leading to *Luciocephalus*, we estimated character states at the beginning (the

earliest stem ancestor, or ESA, of *Luciocephalus* species) and end (the MRCA for *Luciocephalus*) of this branch. Estimation of these ancestral states accounted for differences in evolutionary rates between the *Luciocephalus* lineage and other anabantoids (identified using methods described in the previous section). We estimated the state for the MRCA of *Luciocephalus* under Brownian motion after transforming the branch below it by a factor equal to the ratio of its evolutionary rate to the rate estimated in other anabantoids. When the rate leading to *Luciocephalus* is faster than that of other anabantoids, the branch is lengthened, effectively diminishing the influence of observed states in other anabantoids relative to those of the two *Luciocephalus* species. In contrast, the state of the *Luciocephalus* ESA reflects the evolutionary rate for the rest of the anabantoids and is not conditioned on the observed states in *Luciocephalus* species. Following Felsenstein (1985), the estimated state at this node is the branch length weighted average of the estimated state at the node preceding it and the observed state in the sister node of the *Luciocephalus* MRCA (which is *Sphaerichthys osphromenoides*). Ancestral states were estimated using the *fastAnc* function of *phytools* (Revell 2012). We evaluated the evolutionary trajectory leading to *Luciocephalus* as the ESA-MRCA distance matrix and used its first eigenvector ( $v_L$ ) to describe its orientation in body region morphospace. This

procedure follows the method of Collyer and Adams (2007) and Adams and Collyer (2007, 2009), and our adaptation of the method for reconstructing evolution along a single phylogenetic branch follows Collar et al. (2014).

To estimate the primary axis of body region diversification in non-*Luciocephalus* anabantoids, we removed both *Luciocephalus* species and performed a principal components analysis (PCA) on the phylogenetically controlled covariance matrix of species values for  $A_2$ ,  $H$ ,  $PC$ , and  $C$ . This method follows Revell (2009) and we used the *phytools* function *phyl.pca* (Revell 2012) to implement it. We took PC 1 to be the primary axis of diversification in anabantoids (excluding *Luciocephalus*), and the orientation of this axis in body region morphospace is defined by its eigenvector ( $v_A$ ).

We evaluated whether the observed alignment between the *Luciocephalus* trajectory and the primary axis of anabantoid diversification differed from the alignment expected under the null hypothesis that a constant pattern of multivariate evolution prevailed over all anabantoid lineages. The alignment of these two axes is the angle ( $\theta_{VSI}$ ) between them in body region morphospace:  $\theta_{VSI} = \cos^{-1}[(v_L)'v_A]$  (Pimentel 1979; Schluter 1996). We compared the empirical  $\theta_{VSI}$  to a null distribution based on simulation. Body region states for all 24 anabantoid species (including the two *Luciocephalus* species) were simulated under a Brownian motion model with a constant evolutionary variance-covariance matrix, which was empirically estimated based on the *Luciocephalus*-pruned anabantoid tree and data using the method of Revell and Harmon (2008) implemented in the function *ratematrix* in the *geiger* package (Pennell et al. 2014) for R (R Core Development Team 2015). We then repeated the steps described above to calculate  $\theta_{VSI}$  on the simulated data to obtain its null distribution. The analysis involving the MCC tree used 1000 simulation replicates, whereas analyses performed across the posterior sample of trees used 100 replicates per tree. Simulations were carried out in the *geiger* function *sim.char* (Pennell et al. 2014).

We used a bootstrapping procedure to assess the robustness of the primary axis of anabantoid diversification to the particular sample of species included in the analysis. We subsampled non-*Luciocephalus* anabantoid species at 90, 80, and 70% of the initial species sample size (equal to 20, 18, and 16 non-*Luciocephalus* species) and obtained 100 bootstrap replicates for each level of subsampling. For each bootstrap replicate, we repeated the phylogenetic PCA for anabantoids with *Luciocephalus* excluded using the MCC tree. This analysis resulted in a distribution for the eigenvector of anabantoid PC 1 for each level of subsampling. We also evaluated the alignment between anabantoid PC 1 and the inferred *Luciocephalus* evolutionary trajectory across all bootstrap replicates.

We tested the assumption that the first principal component of body region evolution is constant across non-*Luciocephalus*

anabantoids, which is implicit in our method for comparing the *Luciocephalus* evolutionary trajectory to the primary axis of anabantoid diversification. Anabantoidei is primarily made up of two families that correspond to two major subclades, Anabantidae and Osphronemidae (a third anabantoid family, Helostomatidae, includes only *Helostoma temminckii*). This phylogenetic split reflects a difference in biogeography, with anabantid species primarily distributed across Africa (except for two species of *Anabas*, which are Asian) and osphronemid species found only in Asia (Rüber et al. 2006). The phylogenetic and biogeographic separation between these clades may have led to a difference in primary axes of body region diversification. To evaluate this possibility, we used the method described in the previous section. We performed phylogenetically controlled PCA separately within each clade, and estimated  $\theta_{VSI(Anab,Osph)}$ , the angle between PC 1 for Anabantidae and PC 1 for Osphronemidae. We then compared  $\theta_{VSI(Anab,Osph)}$  to a null distribution derived by simulation under a constant pattern of evolution for both subclades.

## THE ANATOMICAL BASIS OF HEAD ELONGATION

Our analysis revealed that head elongation is of major importance to the body shape transformation in *Luciocephalus*, and so we examined the finer-scale structural changes underlying head shape evolution. For this investigation, we partitioned head length into pre- and postorbital length ( $L_{preorb}$  and  $L_{postorb}$ , respectively) because these aspects of the skull represent different functional regions.  $L_{preorb}$  is the distance between the anteriormost point of the jaws and the anterior margin of the orbit and is mainly made up of the jaws and oral cavity.  $L_{postorb}$  is the distance between the posterior margin of the orbit and the posteriormost point of the operculum and is made up of the opercular region and neurocranium. Combining these terms,

$$H = (L_{preorb} + L_{postorb}) \times AR_H. \quad (2)$$

We note that both  $L_{preorb}$  and  $L_{postorb}$  were evaluated as the number of vertebrae equal to the measured distance between relevant landmarks (e.g.,  $L_{preorb}$  is the linear distance of the preorbital region of the skull divided by the mean length of individual pre-caudal and caudal vertebrae). We used the methods described above to assess the rate of morphological change leading to *Luciocephalus* and to test the alignment between the *Luciocephalus* trajectory and the primary axis of anabantoid diversification in this cranial morphospace ( $\theta_H$ ).

## Results

We found strong evidence that *Luciocephalus* experienced a major transformation in body form.  $VSI$ s for *L. pulcher* and *L. aura* are 2.5 times greater than the next most elongate anabantoid and

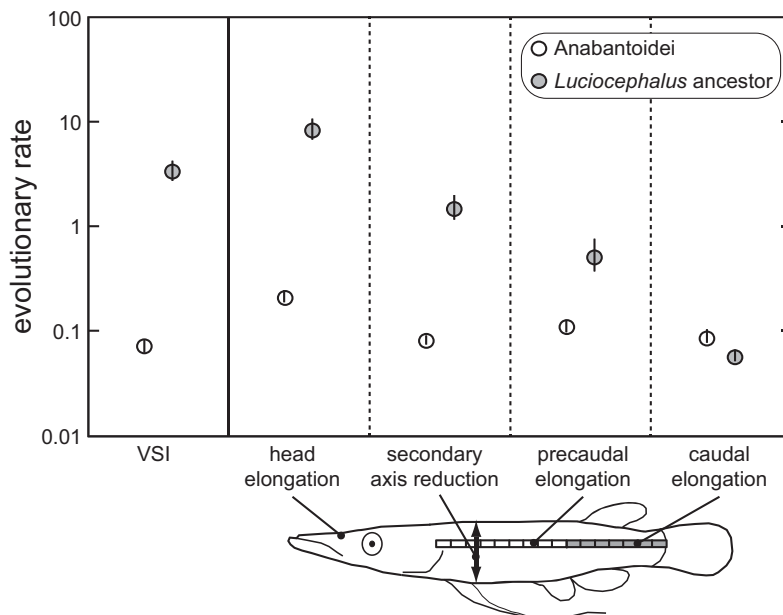


**Figure 2.** Comparison of evolutionary rates for VSI and its anatomical components in ancestral *Luciocephalus* (gray circles) and other anabantoids (white circles). Evolutionary rates are model-averaged estimates based on fitting one- and two-rate Brownian models to species data given the maximum clade credibility tree. Error bars represent the mid-95% intervals based on model-averaged rate estimates from a posterior sample of 100 trees. Body regions are depicted schematically on a line drawing of *L. pulcher*.

more than three times greater than the anabantoid mean (Fig. 1; Table S1). Moreover, the two-rate Brownian model, which allows a unique evolutionary rate on the phylogenetic branch leading to *Luciocephalus* species, was strongly favored over the constant-rate model ( $\Delta\text{AICc} = \text{AICc} [\text{one-rate}] - \text{AICc} [\text{two-rate}] = 14.6$  based on the MCC tree; the mid-95% interval of the distribution of values obtained over posterior sample of trees is [12.1, 17.7]); see Table S2). The *Luciocephalus*-specific rate of VSI evolution is greater than the rate in other anabantoids by a factor of 47 [44, 52] (hereafter the stand-alone value is based on the MCC tree and values in brackets refer to the mid-95% interval obtained over the posterior sample of trees) (Fig. 2). *Luciocephalus* therefore exhibits an extreme form that arose as a consequence of exceptional evolutionary change following its split from other anabantoids.

This body shape transformation is primarily a consequence of head elongation (*H*), though reduction in body depth ( $A_2$ ) and precaudal vertebral elongation (*PC*) also contribute. Head elongation in the two *Luciocephalus* species is four times greater than the next greatest anabantoid (see Table S1), and the evolutionary rate leading to *Luciocephalus* is faster than other anabantoids by a factor of 40 [36, 43] (Fig. 2; Table S2). These differences are less dramatic for  $A_2$  and *PC*, but *L. pulcher* and *L. aura* exhibit extreme values for these components and the rate of evolutionary change in the *Luciocephalus* ancestor is substantially different from what is observed in other anabantoids (Tables S1, S2; Fig. 2). We note that *PC* elongation is primarily driven by an

increase in the number of vertebrae in this axial region with little change in the shape of individual vertebrae (see Fig. S1). Caudal elongation (*C*), on the other hand, contributes little to *Luciocephalus* body elongation. *Luciocephalus* species exhibit *C* values within the range of other anabantoids (Table S1), and the estimated rate of *C* evolution is actually slightly lower in *Luciocephalus* (though not so much lower as to prefer the single-rate over the two-rate model; Table S2). Consistent with these findings, the evolutionary trajectory of *Luciocephalus* in body region morphospace aligns tightly with *H*, moderately with  $A_2$  and *PC*, and negligibly with *C* (Table 1).

The primary axis of body region diversification (i.e., PC 1) in Anabantoidei excluding *Luciocephalus* separates deep-bodied from fusiform species (Fig. 3). Species scores on PC 1 are strongly correlated with their values for VSI ( $r = 0.91$  [0.90, 0.93]). This axis explains 64% [56, 76%] of the variation in evolutionary change among anabantoids and aligns tightly with *H*, moderately with  $A_2$  and *PC*, and minimally with *C* (Table 1). We found little evidence of heterogeneity in the pattern of evolution between the subclades, Anabantidae and Osphronemidae, in spite of their separate evolutionary and biogeographic histories. Although these axes are somewhat oblique to one another ( $\theta_{\text{VSI}(\text{Anab}, \text{Osph})} = 0.82$  [0.78, 0.88]; also see Table S4), angles at least this large occur with moderate probability under constant evolutionary rates and covariances for the two subclades ( $P(\geq \theta_{\text{VSI}(\text{Anab}, \text{Osph})}) = 0.16$  for the MCC tree and for 98% of the posterior sample of trees,  $P(\geq \theta_{\text{VSI}(\text{Anab}, \text{Osph})}) \geq 0.10$ ).

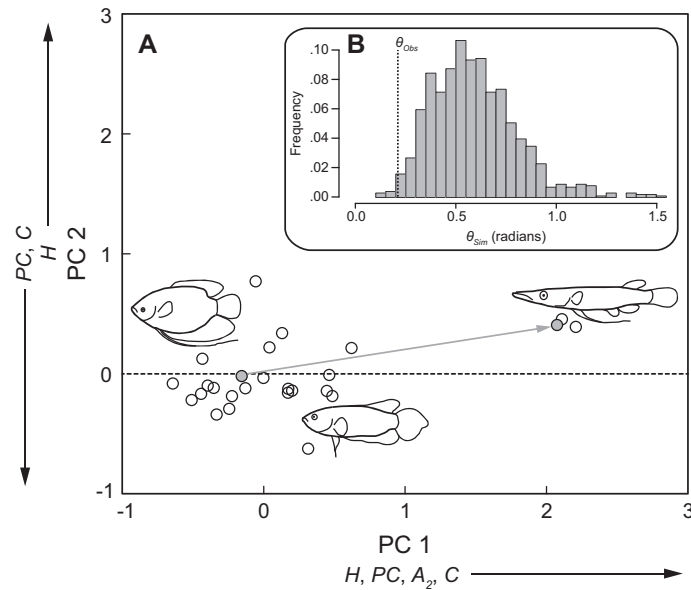


**Figure 3.** (A) Body region morphospace for Anabantoidei and (B) test of the alignment between the *Luciocephalus* evolutionary trajectory and primary axis of diversification in other anabantoids. The morphospace (A) is based on a principal components analysis of the phylogenetically controlled covariance matrix of *VSI*'s body region components for anabantoid species with *Luciocephalus* excluded. Body region component abbreviations are as follows: *H* is head elongation, *A*<sub>2</sub> is reduction of the secondary body axis, *PC* is precaudal elongation, and *C* is caudal elongation. Loadings of body region variables on PCs 1 and 2 are in Table S3, and axis labels show variables with loadings greater than 0.2. To depict the alignment between the *Luciocephalus* evolutionary trajectory and PC 1 of anabantoid evolution, we placed the two *Luciocephalus* species, their most recent common ancestor (MRCA), and their earliest stem ancestor (ESA) into this morphospace. The angle between the *Luciocephalus* trajectory (gray line extending from the *Luciocephalus* ESA to MRCA) and anabantoid PC 1 (horizontal dashed line) is equal to  $\theta_{obs}$  (dashed vertical line in panel B). The histogram (panel B) shows the null distribution for  $\theta$  based on 1000 replicates of simulated Brownian evolution under a constant pattern of multivariate evolution.  $\theta_{obs}$  is less than 98.9% of  $\theta$ s simulated under the constant model.

**Table 1.** Orientation of *VSI* anatomical components on anabantoid PC 1 and the *Luciocephalus* evolutionary trajectory.

Variable	Anabantoid PC 1	<i>Luciocephalus</i> trajectory
2° axis reduction	0.298 ± 0.113	0.386 ± 0.003
Head elongation	0.853 ± 0.094	0.877 ± 0.001
Precaudal elongation	0.399 ± 0.140	0.285 ± 0.002
Caudal elongation	0.156 ± 0.155	0.007 ± 0.005

Coefficient estimates are based on the maximum clade credibility tree. Standard errors for labyrinth PC 1 represent error in coefficient estimation (determined by parametric bootstrapping) and phylogenetic uncertainty. Standard errors for *Luciocephalus* trajectory result from phylogenetic uncertainty.

The evolutionary trajectory of *Luciocephalus* in body region morphospace is closely aligned with the primary axis of diversification in other anabantoids (Fig. 3). The angle between these axes is small ( $\theta_{VSI} = 0.21$  [0.15, 0.24] radians) and lower than 98.9% [95, 100%] of  $\theta$ s estimated across simulation replicates under a constant pattern of evolution in anabantoids (i.e.,  $P(\geq \theta_{VSI}) = 0.989$  [0.95, 1.00] and  $P(\geq \theta_{VSI}) > 0.95$  for 97 of the 100 trees).

Although we implemented this test to detect heterogeneity in the pattern of evolution, these results instead indicate that the *Luciocephalus* trajectory is more closely aligned with anabantoid evolution than expected even when the multivariate pattern of evolution is assumed to be constant in all anabantoid lineages. In other words, the stochastic nature of the Brownian motion process allows for greater deviations in  $\theta_{VSI}$  than we observe.

These results are robust to both phylogenetic uncertainty and species sampling. The eigenvector for anabantoid PC 1 is stable across the posterior sample of phylogenetic trees (Table 1) and across subsamples of anabantoid species (Table S5). Moreover, this axis aligns with the *Luciocephalus* evolutionary trajectory consistently across trees (described in the preceding paragraph) and bootstrap replicates (see Table S5).

The dramatic head elongation in *Luciocephalus* is a consequence of extreme change in all three cranial components. Compared to other anabantoids, *Luciocephalus* has experienced exceptionally rapid evolution in preorbital length ( $L_{preorb}$ ), postorbital length ( $L_{postorb}$ ), and head aspect ratio ( $AR_H$ ), though the most extreme change is in  $L_{preorb}$ , which evolves 57 [51, 63] times faster in the ancestral *Luciocephalus* (Fig. 4; Table S6).

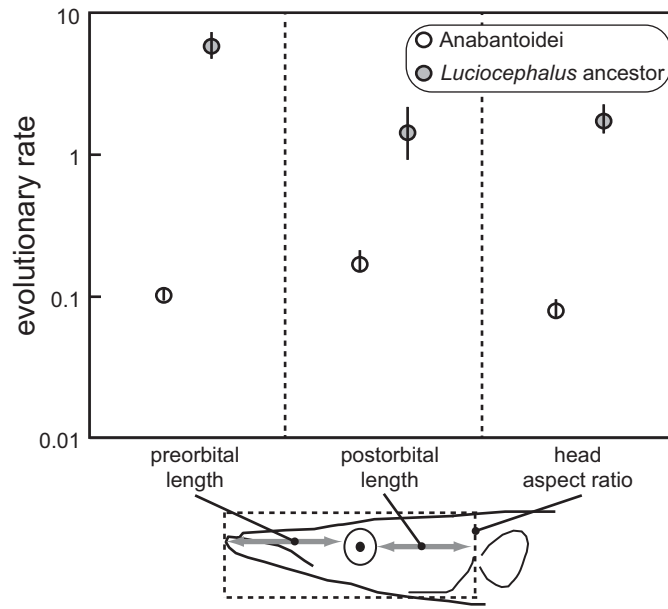


**Figure 4.** Comparison of evolutionary rates for structural components of head shape in ancestral *Luciocephalus* (gray circles) and other anabantoids (white circles). As in Fig. 2, rates are model-averaged estimates given the maximum clade credibility tree, and error bars represent the mid-95% intervals based on rate estimates from a posterior sample of 100 trees. Cranial components are shown schematically on a line drawing of the head of *L. pulcher*.

The evolutionary trajectory of *Luciocephalus* aligns well with the major axis of anabantoid evolution in cranial morphospace ( $\theta_H = 0.486 [0.416, 0.559]$  radians), and angles at least this large occur with moderate probability under a constant pattern of cranial evolution ( $P(\geq \theta_H) = 0.28 [0.14, 0.35]$ ).  $L_{preorb}$  loads strongly on both the *Luciocephalus* trajectory and primary anabantoid axis, though these axes differ somewhat in the loading of  $L_{preorb}$  relative to the other two components (Table 2); in *Luciocephalus*,  $L_{preorb}$  is substantially greater than either  $L_{postorb}$  or  $AR_H$ , but in the other anabantoids,  $L_{postorb}$  is greater than  $L_{preorb}$ .

### Discussion

Bursts of morphological evolution within single species can drastically increase disparity within clades. Identifying the structural changes involved is therefore critical to advancing understanding of the genetic, developmental, and selective factors that promote diversification. However, here we argue that a complete accounting of the anatomical basis of morphological transformation also requires comparison between these structural changes and the pattern of evolution in the clade from which it is derived. Is rapid evolution a consequence of changes in structures that are ancestrally labile or the product of novel combinations of character change? We propose that the answer to this question can help determine whether the evolutionary processes driving extreme changes in form are similar or fundamentally different from those that guide routine between-species divergence. We show that a major transformation in body shape occurs through a burst of

**Table 2.** Orientation of head elongation components on anabantoid PC 1 and the *Luciocephalus* evolutionary trajectory.

Variable	Anabantoid PC 1	<i>Luciocephalus</i> trajectory
Preorbital length	0.653 ± 0.146	0.774 ± 0.003
Postorbital length	0.752 ± 0.202	0.455 ± 0.007
Head aspect ratio	0.082 ± 0.322	0.440 ± 0.003

Coefficient estimates are based on the maximum clade credibility tree. Standard errors for labyrinth PC 1 represent error in coefficient estimation (determined by parametric bootstrapping) and phylogenetic uncertainty. Standard errors for *Luciocephalus* trajectory result from phylogenetic uncertainty.

change along an axis of anatomical evolution that is shared with ancestral and closely related lineages.

Within labyrinth fishes, *Luciocephalus* experienced exceptionally rapid evolution (Fig. 2) from a deep-bodied ancestor to the torpedo shape of *L. aura* and *L. pulcher* (Fig. 1). This transformation results primarily from elongation of the head, but reduction in body depth and lengthening of the precaudal vertebral region are also important (Figs. 2 and 3, Table 1). These anatomical changes define an evolutionary trajectory that aligns closely with the primary axis (i.e., PC 1) of anatomical diversification in other anabantoids (Fig. 3; Table 1). Even the finer-scale structural changes that elongate the skull of *Luciocephalus* show good alignment with the major axis of cranial diversification in other anabantoids (Table 2). Altogether our results suggest that

the body shape transformation in *Luciocephalus* involved change in anatomical features that were ancestrally evolutionarily labile, though the rate of evolution leading to *Luciocephalus* is exaggerated.

This finding suggests that the extreme body shape change in *Luciocephalus* was driven by processes similar to those that govern divergence among other anabantoid species. We consider two nonexclusive explanations: (1) the major axis of extrinsic selection is shared across species and morphological transformation represents a high degree of specialization on this axis, and (2) shared intrinsic constraints (i.e., genetics, development, function) bias the direction of response to selection but not its magnitude. We consider these explanations separately below. But we recognize of course that morphological transformation could result from both a shared axis of selection and common constraints on the response to selection. Indeed, prior studies have suggested that rapid evolution requires alignment of the direction of selection and primary axis of available variation (Schluter 1996; Arnold et al. 2001; Goswami et al. 2014).

(1) *Transformation may represent evolution toward a highly specialized extreme on a shared selective axis.* We speculate that this shared extrinsic selective axis is at least partly related to divergence in trophic ecology between top-level piscivores and mid-level insectivores, which is a common axis of ecological evolution in freshwater fishes (Werner 1974; Keast 1978; Norton and Brainerd 1993). Labyrinth fishes show moderate divergence along this trophic axis, with many species of insectivores (species of *Ctenopoma*, *Betta*, *Trichogaster*; Kottelat et al. 1993; Rainboth 1996) as well as some that combine insects and fish in their diets (climbing gourami [*A. testudineus*; Pethiyagoda 1991], giant gourami [*Osphronemus goramy*; Ukkatawewat 2005], Cape kurper [*Sandelia capensis*; Gosse 1986]). *Luciocephalus*, in contrast, is considered primarily piscivorous (Lauder and Liem 1981), and as we argue below, natural selection related to specialization on this diet could have plausibly contributed to the large and rapid morphological changes documented in this lineage.

Trophic variation can impose differing selective demands on a suite of morphological characteristics pertaining to predatory behaviors, swimming abilities, and strike mechanics. Prey types (aquatic insect larvae vs. fish) contrast in predator avoidance tactics and occur in habitats that differ in key characteristics, such as amount of vegetative cover and proximity to substrates. For example, aquatic insects are often found in covered areas attached to substrates or vegetation, and insectivorous freshwater fishes tend to possess relatively deep bodies to enhance maneuverability in structurally complex habitats (Webb 1984) as well as short, stout skulls and jaws to generate strong suction to dislodge prey (Holzman et al. 2011). In contrast, capturing elusive prey, such as other fish, generally requires that the predator swims rapidly while engulfing a large volume of water containing the prey (referred to

as ram feeding), and this strike behavior is often associated with a more streamlined body and longer and more kinetic skulls and jaws (Keast 1978; Norton and Brainerd 1993; Collar et al. 2009; Holzman et al. 2011). In other words, variation between deep-bodied and fusiform shapes may be related to prey-imposed demands for accurate strikes with strong suction versus ram feeding with large ingested volumes (Norton and Brainerd 1993; Higham et al. 2006; Ferry et al. 2012). Indeed, morphological variation in labyrinth fishes is consistent with these patterns. Species that are known to consume at least some fish—*A. testudineus*, *O. goramy*, and *S. capensis*—have relatively large *VSI* and head elongation (*H*) values; these three species fall within the largest 25% of the labyrinth *VSI* and *H* distributions (Table S1). However, we note that dietary information is sparse for many of our sampled species. We were unable to find dietary information on labyrinth species with *VSI* or *H* values near or greater than these three species, and we may have failed to identify other moderately piscivorous species.

The extreme evolutionary change in body shape leading to *Luciocephalus* can be interpreted as highly specialized adaptation to piscivory. The torpedo shape of *Luciocephalus* is shared with other teleost fishes—such as barracuda (Sphyraenidae), needlefish (Belontiidae), and pike (Esocidae)—all of which use a specialized ambush type of ram feeding (Skadsen and Webb 1980; Rand and Lauder 1981; Porter and Motta 2004). Like these species, *Luciocephalus* generates minimal suction and instead uses rapid body acceleration and a large gape—enhanced by extreme cranial elevation—to overtake its prey (Lauder and Liem 1981). Reduction of the secondary body axis and axial elongation provide a long, flexible body that enhances strike acceleration to overtake evasive prey (Webb and Skadsen 1980; Rand and Lauder 1981; Harper and Blake 1991). Moreover, the preferential elongation of the precaudal axial region (vs. the caudal region) in *Luciocephalus* is also seen in a variety of other ambush-striking fishes (Maxwell and Wilson 2013), suggesting that an elongated abdominal region is functionally important to generating the characteristic s-shaped axial bending employed during the initial phase of the strike (Skadsen and Webb 1980; Harper and Blake 1991; Porter and Motta 2004).

The changes in head morphology in *Luciocephalus* also represent extreme adaptations to piscivory. Lengthening the skull increases the out-lever of the epaxial muscles, which power cranial elevation, and increases displacement of the expanding oral cavity but comes at a cost to suction production (Carroll et al. 2004). The dramatic increase in cranial length in *Luciocephalus* likely enhances oral cavity expansion, but the reduction in suction capacity presumably has little effect on prey capture because of behavioral adaptations, like rapid swimming to engulf the prey. In addition, the substantial increase in the preorbital region of the skull in *Luciocephalus* is likely related to its remarkable

capacity to protrude its jaws nearly 33% of the length of its skull (Lauder and Liem 1981), which is a mechanism for enhancing strike speed that has evolved repeatedly in teleost fishes (Waltzek and Wainwright 2003; Westneat 2006). The morphological transformation of *Luciocephalus* therefore reflects anatomical changes associated with piscivory taken to the extreme.

Although we suggest that *Luciocephalus* has evolved in response to a selective axis shared with other labyrinth fishes, we note some limitations to this inference. First, the morphological transition in *Luciocephalus* is unreplicated within Anabantoidei, and as with any unique evolutionary event, identification of causal factors is challenging. A number of ecological or intrinsic features specific to *Luciocephalus* could have contributed to the selective circumstances that drove its remarkable change in body shape. One possibility is an ontogenetic shift. Adult morphology can be strongly influenced by selective demands on juvenile form, and a shift in selection on early life stages (e.g., a change in juvenile habitat use) could also facilitate morphological transformation, though we note that we were unable to find sufficient data to evaluate this hypothesis for labyrinth fishes. Nevertheless, our suggestion that diet is a primary contributor to *Luciocephalus*'s morphological transformation is based on a solid foundation of prior work showing the feeding performance consequences of the underlying anatomical changes. Second, we note that dietary information for labyrinth fishes is limited. Even though some species are known to capture fish at least occasionally, the scarcity of data on feeding habits prevents us from quantitatively investigating broader effects of piscivory in Anabantoidei. Finally, we acknowledge that our method for inferring the evolutionary trajectory of *Luciocephalus* assumes a linear path from its ESA to the MRCA of the two *Luciocephalus* species. However, this path could have instead been nonlinear such that anatomical changes occurred at different times during the history of the lineage, as can occur during adaptive evolution when the primary axis of phenotypic variation does not line up with the direction of the selective optimum (Schluter 1996; Arnold et al. 2001). In this case, some characters may change rapidly early in the lineage's history, whereas others change later or more gradually. Our phylogenetic comparative method is incapable of detecting such a nonlinear accrual of anatomical changes, but we note that the inferred linear trajectory will nevertheless be informative about the main direction of adaptation when the trajectory endpoint is at or near an adaptive peak.

(2) *Shared intrinsic constraints bias the direction of morphological transformation.* Although the selective demands of piscivory were likely important in transforming *Luciocephalus*, the exact combination of anatomical features that evolved in response to this selection may have been influenced by intrinsic constraints shared broadly among labyrinth fishes. In general, response to selection is guided by the available within-species phenotypic

variation and covariation, which are shaped by genetic variances and correlations (Schluter 1996; Houle and Hansen 2008) as well as developmental and functional constraints (Olson and Miller 1965; Klingenberg 2008). Although we do not have sufficient sample sizes to assess the degree to which the primary axis of anabantoid body shape evolution aligns with within-species variation and covariation, prior studies of elongate body form provide some insights into the importance of potential evolutionary constraints acting on different regions of the body.

A question arising from our results is why so much of anabantoid body shape evolution is related to changes in the head rather than the axial skeleton. We are aware of no study that directly compares evolvability of cranial and vertebral morphology, and we are reluctant to speculate on the roles of genetic, developmental, or functional constraints in shaping this pattern. However, we note that in many ray-finned fishes, head elongation contributes less than axial elongation to body shape variation (Collar et al. 2013; Claverie and Wainwright 2014), and anabantoids provide a counterexample to the more widespread pattern. Our results suggest the possibility that in anabantoids head shape is freer to evolve, while vertebral lengthening, particularly in the caudal region, is more constrained.

Caudal elongation contributes relatively little to the primary axis of body shape diversification in anabantoids and even less to the transformation in *Luciocephalus* (Table 1). This result is somewhat surprising because prior studies have found that axial elongation in ray-finned fishes is most tightly associated with an increase in the number of caudal vertebrae (Ward and Brainerd 2007; Ward and Mehta 2010; but see Yamahira and Yashida 2009; Maxwell and Wilson 2013). Instead, anabantoid body shape variation is more strongly associated with lengthening of the precaudal region (Fig. 2, Table 1), which is a result of an increase in the number of vertebrae in this axial region (Fig. S1). This contrast is partly a consequence of developmental processes that allow vertebral numbers in the two axial regions to vary independently. Increasing the number of caudal vertebrae generally results from tail bud extension by increasing the rate of somitogenesis (i.e., segmentation of the paraxial mesoderm that gives rise to the vertebrae) relative to the overall rate of development (Gomez et al. 2008). The number of precaudal vertebrae depends on the location of the precaudal–caudal boundary, which is determined by the anterior limit of the *hox12* expression domain (Burke et al. 1995; van der Hoeven et al. 1996). We speculate that the greater importance of precaudal lengthening in anabantoids is associated with greater variation among species in the latter process. However, even though the precaudal vertebral region contributes more than the caudal region to axial lengthening, its evolution is also likely constrained because it is structurally linked to the abdominal cavity and digestive system. Changes in precaudal length are associated with changes in gut length and digestive efficiency

(Ward and Kley 2012), and trade-offs could potentially exist between mechanics of the precaudal axial skeleton and digestive function.

### ANABANTOID BODY SHAPE IN COMPARISON TO OTHER RAY-FINNED FISHES

The morphological transformation in *Luciocephalus* is extreme within Anabantoidei, but is it remarkable relative to body shape variation in other ray-finned fishes? Comparing anabantoids to data we collected as part of a prior study (Collar et al. 2013), we find that the ancestral *Luciocephalus* evolved from one extreme of the ray-finned fish body shape range to the other. The most deep-bodied anabantoids ( $VSI < 40$ , which includes the sister species to *Luciocephalus*, *S. osphromenoides*, among several others, see Table S1) have  $VSI$ s at the low extreme near coral reef fishes, such as butterflyfish (*Chaetodon multicinctus*,  $VSI = 39.6$ ), and other deep-bodied freshwater fishes, like the scat (*Scatophagus argus*,  $VSI = 38.1$ ). On the other hand, *L. pulcher* ( $VSI = 153.1$ ) and *L. aura* ( $VSI = 163.2$ ) possess  $VSI$ s similar to another pike-like species from the New World freshwater Characiformes, the pike characin (*B. lateristriga*,  $VSI = 166.3$ ), and these species even exceed  $VSI$ s of some eel (e.g., *Anguilla bicolor*,  $VSI = 146.3$ ) and eel-like species (e.g. *Lycodes brevipes* [shortfin eelpout],  $VSI = 115.0$ ). The evolutionary change leading to *Luciocephalus* is indeed remarkable in the context of the range of body shape variation in these other ray-finned fishes.

Our results indicate that the *Luciocephalus* anatomical evolutionary trajectory aligns with the primary axis of diversification in Anabantoidei, but we suspect that this axis is not shared widely across other ray-finned fish groups. As we mention above, body elongation is often associated with large increases in vertebral number, especially in the caudal axial region (Ward and Brainerd 2007), whereas our data reveal that head elongation contributes more strongly than axial elongation to body shape changes in anabantoids. In addition, the precaudal region contributes more than the caudal region to the *Luciocephalus* body shape change, though interestingly, the preferential lengthening of the precaudal region also occurs in several other fish lineages that evolve similar torpedo-shaped bodies (e.g., pike, barracuda, gar, and trumpetfish; see Maxwell and Wilson 2013). Moreover, in a comprehensive comparative study of body shape in coral reef teleost fish families, Claverie and Wainwright (2014) found that families differ with respect to which body regions contribute to elongation, with only a subset showing major contributions from head lengthening. Our study not only contributes to a growing body of knowledge regarding what anatomical changes are responsible for the incredible diversity of fish shapes, but we are the first that we know of to show that body shape transformation can occur along an anatomical axis shared with the clade that gave rise to it. Additional data, especially on internal skeletal anatomy, and phylogenetic

comparative analyses similar to those employed here will be key in determining whether this result is a general feature of body shape diversification across ray-finned fishes and other vertebrates.

### ACKNOWLEDGMENTS

We are grateful to Pan Ocean Aquarium, Inc. for help locating anabantoid specimens. We thank K. Hartel and A. Williston of the Museum of Comparative Zoology (Harvard University) for loaning specimens and providing high-quality digital radiographs. V. Baliga, L. Miller, J. Sharick, and D. Pruitt prepared specimens. This work was funded by an NSF REU grant to RSM. DCC was partially funded by NSF grant DEB 1350474 to L. Revell (University of Massachusetts Boston) during this project.

### DATA ARCHIVING

The doi for our data is <http://dx.doi.org/10.5061/dryad.2d7km>.

### LITERATURE CITED

- Adams, D. C., and M. L. Collyer. 2007. Analysis of character divergence along environmental gradients and other covariates. *Evolution* 61:510–515.
- . 2009. A general framework for the analysis of phenotypic trajectories in evolutionary studies. *Evolution* 63:1143–1154.
- Arnold, S. J., M. E. Pfrender, and A. G. Jones. 2001. The adaptive landscape as a conceptual bridge between micro- and macroevolution. *Genetica* 112–113:9–32.
- Bergmann, P. J., and D. J. Irschick. 2012. Vertebral evolution and diversification of squamate reptiles. *Evolution* 66:1044–1058.
- Bergmann P. J., J. J. Myers, and D. J. Irschick. 2009. Directional evolution of stockiness coevolves with ecology and locomotion in lizards. *Evolution* 63:215–227.
- Brandley, M. C., J. P. Huelsenbeck, and J. J. Wiens. 2008. Rates and patterns in the evolution of snake-like body form in squamate reptiles: evidence for repeated re-evolution of lost digits and long-term persistence of intermediate body forms. *Evolution* 62:2042–2064.
- Britz, R. 1994. Ontogenetic features of *Luciocephalus* (Perciformes, Anabantoidei) with a revised hypothesis of anabantoid interrelationships. *Zool. J. Linn. Soc.* 112:491–508.
- Burke, A. C., C. E. Nelson, B. A. Morgan, and C. Tabin. 1995. Hox genes and the evolution of vertebrate axial morphology. *Development* 121:333–346.
- Burnham, K. P., and D. R. Anderson. 2002. Model selection and mixed model inference: a practical information-theoretic approach. Springer, New York.
- Carroll, A. M., P. C. Wainwright, S. H. Huskey, D. C. Collar, and R. G. Turingan. 2004. Morphology predicts suction feeding performance in centrarchid fishes. *J. Exp. Biol.* 207:3873–3881.
- Claverie, T., and P. C. Wainwright. 2014. A morphospace for reef fishes: elongation is the dominant axis of body shape evolution. *PLoS One* 9:e112732.
- Collar, D. C., B. C. O'Meara, P. C. Wainwright, and T. J. Near. 2009. Piscivory limits diversification of feeding morphology in centrarchid fishes. *Evolution* 63:1557–1573.
- Collar, D. C., J. A. Schulte II, B. C. O'Meara, and J. B. Losos. 2010. Habitat use affects morphological diversification in dragon lizards. *J. Evol. Biol.* 23:1033–1049.
- Collar, D. C., C. M. Reynaga, A. B. Ward, and R. S. Mehta. 2013. A revised metric for quantifying body shape in vertebrates. *Zoology* 116:246–257.
- Collar, D. C., J. S. Reece, M. E. Alfaro, P. C. Wainwright, and R. S. Mehta. 2014. Imperfect morphological convergence: variable changes in cranial

- structures underlie transitions to durophagy in moray eels. *Am. Nat.* 183:E168–E184.
- Collar, D. C., M. Quintero, B. Buttler, A. B. Ward, and R. S. Mehta. 2016. Data from: Body shape transformation along a shared axis of anatomical evolution in labyrinth fishes (Anabantoidei). Dryad Digital Repository. <http://dx.doi.org/10.5061/dryad.2d7km>.
- Collyer, M. L., and D. C. Adams. 2007. Analysis of two-state multivariate phenotypic change in ecological studies. *Ecology* 88:683–692.
- Davidson, E. H., and D. H. Erwin. 2006. Gene regulatory networks and the evolution of animal body plans. *Science* 311:796–800.
- Drummond, A. J., and A. Rambaut. 2007. BEAST: Bayesian evolutionary analysis by sampling trees. *BMC Evol. Biol.* 7:214.
- Drummond A. J., S. Y. W. Ho, M. J. Phillips, and A. Rambaut. 2006. Relaxed phylogenetics and dating with confidence. *PLoS Biol.* 44:88.
- Felsenstein, J. 1985. Phylogenies and the comparative method. *Am. Nat.* 125:1–15.
- Ferry, L. A., N. Konow, and A. C. Gibb. 2012. Are Kissing Gourami specialized for substrate-feeding? Prey capture kinematics in *Helostoma temminckii* and other anabantoid fishes. *J. Exp. Zool.* 317A:571–579.
- Futuyma, D. J. 1987. On the role of species in anagenesis. *Am. Nat.* 130:465–473.
- Gans, C. 1975. Tetrapod limblessness: evolution and functional corollaries. *Am. Zool.* 15:455–467.
- Gomez, C., E. M. Özbudak, J. Wunderlich, D. Baumann, J. Lewis, and O. Pourquié. 2008. Control of somite number in vertebrate embryos. *Nature* 454:335–339.
- Gosse, J. P. 1986. Anabantidae. Pp. 402–414 in J. Daget, J. P. Gosse, and D. F. E. Thys van den Audenaerde, eds. Checklist of the freshwater fishes of Africa. ISBN, Brussels.
- Goswami, A., J. B. Smaers, C. Soligo, and P. D. Polly. 2014. The macroevolutionary consequences of phenotypic integration: from development to deep time. *Philos. Trans. R. Soc. B* 369:20130254.
- Grande, L., and W. E. Bemis. 1998. A comprehensive phylogenetic study of amiid fishes (Amiidae) based on comparative skeletal anatomy. An empirical search for interconnected patterns of natural history. *J. Vert. Paleont.* 18:1–690.
- Gray, L. E. 1831. XIII. Description of twelve new genera of fish, discovered by Gen. Hardwicke, in India, the greater part in the British Museum. *Zool. Miscell.* 1831:7–10.
- Hansen, T. F., and D. Houle. 2008. Measuring and comparing evolvability and constraint in multivariate characters. *J. Evol. Biol.* 21:1201–1219.
- Harper, D. G., and R. W. Blake. 1991. Prey capture and the fast-start performance of Northern Pike, *Esox lucius*. *J. Exp. Biol.* 155:175–192.
- Higham, T. E., S. W. Day, and P. C. Wainwright. 2006. Multidimensional analysis of suction feeding performance in fishes: fluid speed, acceleration, strike accuracy and the ingested volume of water. *J. Exp. Biol.* 209:2713–2725.
- Hohenlohe, P. A., and S. J. Arnold. 2008. MIPoD: a hypothesis-testing framework for microevolutionary inference from patterns of divergence. *Am. Nat.* 171:366–385.
- Holzman, R., D. C. Collar, R. S. Mehta, and P. C. Wainwright. 2011. Functional complexity can mitigate performance trade-offs. *Am. Nat.* 177:E69–E83.
- Huelsenbeck, J. P., and B. Rannala. 2003. Detecting correlation between characters in a comparative analysis with uncertain phylogeny. *Evolution* 57:1237–1247.
- Jansen, G., S. Davaere, P. H. H. Weekers, and D. Adriaens. 2006. Phylogenetic relationships and divergence time estimate of African anguilliform catfish (Siluriformes: Clariidae) inferred from ribosomal gene and spacer sequences. *Mol. Phylogenet. Evol.* 38:65–78.
- Keast, A. 1978. The piscivore feeding guild of fishes in small freshwater ecosystems. *Environ. Biol. Fish.* 12:119–129.
- Klingenberg, C. P. 2008. Morphological integration and developmental modularity. *Annu. Rev. Ecol. Syst.* 39:115–132.
- Kottelat, M., A. J. Whitten, S. N. Kartikasari, and S. Wirjoatmodjo. 1993. Freshwater fishes of Western Indonesia and Sulawesi. Periplus Editions, Hong Kong.
- Kozak, K. H., D. W. Weisrock, and A. Larson. 2006. Rapid lineage accumulation in a non-adaptive radiation: phylogenetic analysis of diversification rates in eastern North American woodland salamanders (Plethodontidae, *Plethodon*). *Proc. R. Soc. Lond. B* 273:539–546.
- Lauder, G. V., and K. F. Liem. 1981. Prey capture by *Luciocephalus pulcher*: implications for models of jaw protrusion in teleost fishes. *Environ. Biol. Fish.* 6:257–268.
- . 1983. The evolution and interrelationships of the actinopterygian fishes. *Bull. Mus. Comp. Zool.* 150:95–197.
- Liem, K. F. 1980. Air ventilation in advanced teleosts: biomechanical and evolutionary aspects. Pp. 57–91 in M. A. Ali, ed. Environmental physiology of fishes. Plenum Press, New York.
- Losos, J. B. 2009. Lizards in an evolutionary tree: ecology and adaptive radiation of anoles. Univ. California Press, Berkeley, CA.
- Mahler, D. L., L. J. Revell, R. E. Glor, and J. B. Losos. 2010. Ecological opportunity and the rate of morphological evolution in the diversification of Greater Antillean anoles. *Evolution* 64:2731–2745.
- Martin, C. P. and P. C. Wainwright. 2011. Trophic novelty is linked to exceptional rates of morphological diversification in two adaptive radiations of *Cyprinodon* pupfishes. *Evolution* 65:2197–2212.
- Maxwell, E. E., and L. A. B. Wilson. 2013. Regionalization of the axial skeleton in the “ambush predator” guild—are there developmental rules underlying body shape evolution in ray-finned fishes? *BMC Evol. Biol.* 13:265.
- Mayr, E. 1963. Animal species and evolution. Harvard Univ. Press, Cambridge, U.K.
- McPeck, M. A. 1995. Testing hypotheses about evolutionary change on single branches of a phylogeny using evolutionary contrasts. *Am. Nat.* 145:686–703.
- Mehta, R. S., and P. C. Wainwright. 2007. Raptorial jaws in the throat help moray eels swallow large prey. *Nature* 449:79–83.
- Mehta, R. S., A. B. Ward, M. E. Alfaro, and P. C. Wainwright. 2010. Elongation of the body in eels. *Integr. Comp. Biol.* 50:1091–1105.
- Nelson, J. S. 2006. Fishes of the world. 4th ed. John Wiley and Sons, New York.
- Norton, S. F., and E. L. Brainerd. 1993. Convergence in the feeding mechanics of ecomorphologically similar species in the Centrarchidae and Cichlidae. *J. Exp. Biol.* 176:11–29.
- Olson, E. C., and R. L. Miller. 1965. Morphological integration. Univ. Chicago Press, Chicago.
- O’Meara, B. C., C. Ané, M. J. Sanderson, P. C. Wainwright. 2006. Testing for different rates of continuous trait evolution using likelihood. *Evolution* 60:922–933.
- Parra-Olea, G., and D. B. Wake. 2001. Extreme morphological and ecological homoplasy in tropical salamanders. *Proc. Natl. Acad. Sci. USA* 98:7888–7891.
- Pennell, M. W., J. M. Eastman, G. J. Slater, J. W. Brown, J. C. Uyeda, R. G. Fitzjohn, M. E. Alfaro, and L. J. Harmon. 2014. geiger v2.0: an expanded suite of methods for fitting macroevolutionary models to phylogenetic trees. *Bioinformatics* 30:2216–2218.
- Peters, H. M. 1978. On the mechanism of air ventilation in anabantoids (Pisces: Teleostei). *Zoomorphology* 89:93–123.
- Pethiyagoda, R. 1991. Freshwater fishes of Sri Lanka. The Wildlife Heritage Trust of Sri Lanka, Colombo.

- Pimentel, R. A. 1979. Morphometrics. Kendall/Hunt, Dubuque, IA.
- Porter, H. T., and P. J. Motta. 2004. A comparison of strike and prey capture kinematics of three species of piscivorous fishes: Florida gar (*Lepisosteus platyrhincus*), redbfin needlefish (*Strongylura notata*), and great barracuda (*Sphyraena barracuda*). *Mar. Biol.* 145:989–1000.
- Price, S. A., P. C. Wainwright, D. R. Bellwood, E. Kazancioglu, D. C. Collier, and T. J. Near. 2010. Functional innovations and morphological diversification in parrotfish. *Evolution* 64:3057–3068.
- Price, S. A., R. Holzman, T. J. Near, and P. C. Wainwright. 2011. Coral reefs promote the evolution of morphological diversity and ecological novelty in labrid fishes. *Ecol. Lett.* 14:462–469.
- R Core Development Team. 2015. R: a language and environment for statistical computing. R Foundation for Statistical Computing, Vienna, Austria.
- Rainboth, W. J. 1996. Fishes of the Cambodian Mekong. FAO species identification field guide for fishery purposes. Food and Agriculture Organization of the United States, Rome.
- Rand, D. M., and G. V. Lauder. 1981. Prey capture in the chain pickerel, *Esox niger*: correlations between feeding and locomotor behavior. *Can. J. Zool.* 59:1072–1078.
- Revell, L. J. 2008. On the analysis of evolutionary change along single branches in a phylogeny. *Am. Nat.* 172:140–147.
- . 2009. Size-correction and principal components for interspecific comparative studies. *Evolution* 63:3258–3268.
- . 2012. phytools: an R package for phylogenetic comparative biology (and other things). *Methods Ecol. Evol.* 3:217–223.
- Revell, L. J., and L. J. Harmon. 2008. Testing quantitative genetic hypotheses about the evolutionary rate matrix for continuous characters. *Evol. Ecol. Res.* 10:311–331.
- Ricklefs, R. E. 2005. Small clades at the periphery of passerine morphospace. *Am. Nat.* 165:651–659.
- Rüber, L., R. Britz, and R. Zardoya. 2006. Molecular phylogenetics and evolutionary diversification of labyrinth fishes (Perciformes: Anabantoidae). *Syst. Biol.* 55:374–397.
- Schluter, D. 1996. Adaptive radiation along genetic lines of least resistance. *Evolution* 50:1766–1774.
- Seehausen, O. 2006. African cichlid fish: a model system in adaptive radiation research. *Proc. R. Soc. B* 273:1987–1998.
- Simpson, G. G. 1953. The major features of evolution. Columbia Univ. Press, New York.
- Song, J., and L. R. Parenti. 1995. Clearing and staining whole fish specimens for simultaneous demonstration of bone, cartilage, and nerves. *Copeia* 1995:114–118.
- Steppan, S. J., P. C. Phillips, and D. Houle. 2002. Comparative quantitative genetics: evolution of the G matrix. *Trends Ecol. Evol.* 17:320–327.
- Ukkatawewat, S. 2005. The taxonomic characters and biology of some important freshwater fishes in Thailand. National Inland Fisheries Institute, Department of Fisheries, Ministry of Agriculture, Bangkok, Thailand.
- van der Hoeven, F., P. Sordino, N. Fraudeau, J.-C. Izpisua-Belmonte, and D. Duboule. 1996. Teleost *HoxD* and *HoxA* genes: a comparison with tetrapods and functional evolution of the *HOXD* complex. *Mech. Dev.* 54:9–21.
- Wagner, C. E., L. J. Harmon, and O. Seehausen. 2012. Ecological opportunity and sexual selection together predict adaptive radiation. *Nature* 487:366–370.
- Wake, D. B. 1966. Comparative osteology and evolution of the lungless salamander, Family Plethodontidae. *Mem. South. Calif. Acad. Sci.* 4:1–111.
- Wake, D. G., G. Roth, and M. H. Wake. 1983. On the problem of stasis in organismal evolution. *J. Theor. Biol.* 101:211–224.
- Wake, M. H. 1980. Morphometrics of the skeleton of *Dermophis mexicanus* (Amphibia: Gymnophiona). Part I. The vertebrae, with comparisons to other species. *J. Morphol.* 165:117–130.
- Waltzek, T. B., and P. C. Wainwright. 2003. Functional morphology of extreme jaw protrusion in Neotropical cichlids. *J. Morphol.* 257:96–106.
- Ward, A. B., and E. L. Brainerd. 2007. Evolution of axial patterning in elongate fishes. *Biol. J. Linn. Soc.* 90:97–116.
- Ward, A. B., and N. J. Kley. 2012. Effects of precaudal elongation on visceral topography in a basal clade of ray-finned fishes. *Anat. Rec.* 295:289–297.
- Ward, A. B., and R. S. Mehta. 2010. Axial elongation in fishes: using morphological approaches to elucidate developmental mechanisms in studying body shape. *Integr. Comp. Biol.* 50:110–1119.
- Webb, P. W. 1982. Locomotor patterns in the evolution of actinopterygian fishes. *Am. Zool.* 22:329–342.
- Webb, P. W. 1984. Body form, locomotion and foraging in aquatic vertebrates. *Am. Zool.* 24:107–120.
- Webb, P. W., and J. M. Skadsen. 1980. Strike tactics of *Esox*. *Can. J. Zool.* 58:1462–1469.
- Werner, E. E. 1974. The fish size, prey size, handling time relation in several sunfishes and some implications. *J. Res. Board Canada* 31:1531–1536.
- Westneat, M. W. 2006. Skull biomechanics and suction feeding in fishes. Pp. 29–75 in G. V. Lauder and R. E. Shadwick, eds. *Fish biomechanics*. Elsevier Academic Press, San Diego.
- Wiens, J. J., and J. L. Singluff. 2001. How lizards turn into snakes: a phylogenetic analysis of body-form evolution in anguillid lizards. *Evolution* 55:2303–2318.
- Wiens, J. J., M. C. Brandley, and T. W. Reeder. 2006. Why does a trait evolve multiple times within a clade? Repeated evolution of snakelike body form in squamate reptiles. *Evolution* 60:123–141.
- Yamada, T., T. Sugiyama, N. Tamaki, A. Kawakita, and M. Kato. 2009. Adaptive radiation of gobies in the interstitial habitats of gravel beaches accompanied by body elongation and excessive vertebral segmentation. *BMC Evol. Biol.* 9:145.
- Yamahira, K., and T. Nishida. 2009. Latitudinal variation in axial patterning of the medaka (Actinopterygii: Adrianichthyidae): Jordan's rule is substantiated by genetic variation in abdominal vertebral number. *Biol. J. Linn. Soc.* 96:856–866.

Associate Editor: M. Friedman  
Handling Editor: J. Conner

## Supporting Information

Additional Supporting Information may be found in the online version of this article at the publisher's website:

**Table S1.** Sampling and species means for *VSI* and its anatomical components.

**Table S2.** Model selection summary for *VSI* and its anatomical components.

**Table S3.** Loadings of body region variables on anabantoid PCs 1 and 2, as depicted in Figure 3.

**Table S4.** Orientation of *VSI* anatomical variables on PC 1 for Anabantidae and Osphronemidae.

**Table S5.** Major axis of anabantoid diversification, evolutionary trajectory for *Luciocephalus*, and their alignment across varying species sample sizes.

**Table S6.** Model selection summary for the structural variables comprising head elongation.

**Figure S1.** Comparison of evolutionary rates for components of axial elongation in ancestral *Luciocephalus* (gray circles) and other anabantoids (white circles).